

Article

Stress Responses and Ammonia Nitrogen Removal Efficiency of *Oocystis lacustris* in Saline Ammonium-Contaminated Wastewater Treatment

Yuqi Zhu ¹, Yili Zhang ¹, Hui Chen ², Lisha Zhang ¹ and Chensi Shen ^{1,*}

¹ College of Environmental Science and Engineering, Donghua University, Shanghai 201620, China; 18017207003@163.com (Y.Z.); 17792797372@163.com (Y.Z.); lszhang@dhu.edu.cn (L.Z.)

² Key Laboratory of Agricultural Germplasm Resources Mining and Environmental Regulation of Ningbo City, College of Science and Technology, Ningbo University, Cixi 315302, China; chenhui07@126.com

* Correspondence: shencs@dhu.edu.cn

Abstract: The increasing concern over climate change has spurred significant interest in exploring the potential of microalgae for wastewater treatment. Among the various types of industrial wastewaters, high-salinity $\text{NH}_4^+\text{-N}$ wastewater stands out as a common challenge. Investigating microalgae's resilience to $\text{NH}_4^+\text{-N}$ under high-salinity conditions and their efficacy in $\text{NH}_4^+\text{-N}$ utilization is crucial for advancing industrial wastewater microalgae treatment technologies. This study evaluated the effectiveness of employing nitrogen-efficient microalgae, specifically *Oocystis lacustris*, for $\text{NH}_4^+\text{-N}$ removal from saline wastewater. The results revealed *Oocystis lacustris*'s tolerance to a Na_2SO_4 concentration of 5 g/L. When the Na_2SO_4 concentration reached 10 g/L, the growth inhibition experienced by *Oocystis lacustris* began to decrease on the 6th day of cultivation, with significant alleviation observed by the 7th day. Additionally, the toxic mechanism of saline $\text{NH}_4^+\text{-N}$ wastewater on *Oocystis lacustris* was analyzed through various parameters, including chlorophyll-a, soluble protein, oxidative stress indicators, key nitrogen metabolism enzymes, and microscopic observations of algal cells. The results demonstrated that when the *Oocystis lacustris* was in the stationary growth phase with an initial density of 2×10^7 cells/L, $\text{NH}_4^+\text{-N}$ concentrations of 1, 5, and 10 mg/L achieved almost 100% removal of the microalgae on the 1st, 2nd, and 4th days of treatment, respectively. On the other hand, saline $\text{NH}_4^+\text{-N}$ wastewater minimally impacted photosynthesis, protein synthesis, and antioxidant systems within algal cells. Additionally, $\text{NH}_4^+\text{-N}$ within the cells was assimilated into glutamic acid through glutamate dehydrogenase-mediated pathways besides the conventional pathway involving $\text{NH}_4^+\text{-N}$ conversion into glutamine and assimilation amino acids.

Keywords: saline $\text{NH}_4^+\text{-N}$ wastewater; microalgae treatment technology; *Oocystis lacustris*; $\text{NH}_4^+\text{-N}$ utilization; stress responses



Citation: Zhu, Y.; Zhang, Y.; Chen, H.; Zhang, L.; Shen, C. Stress Responses and Ammonia Nitrogen Removal Efficiency of *Oocystis lacustris* in Saline Ammonium-Contaminated Wastewater Treatment. *Toxics* **2024**, *12*, 353. <https://doi.org/10.3390/toxics12050353>

Academic Editor: Mark Taggart

Received: 21 March 2024

Revised: 24 April 2024

Accepted: 8 May 2024

Published: 10 May 2024



Copyright: © 2024 by the authors. Licensee MDPI, Basel, Switzerland. This article is an open access article distributed under the terms and conditions of the Creative Commons Attribution (CC BY) license (<https://creativecommons.org/licenses/by/4.0/>).

1. Introduction

Water eutrophication, resulting from an excess of nitrogen, phosphorus, and other nutrients in water, poses a threat to water resources worldwide [1,2]. Ammonia nitrogen ($\text{NH}_4^+\text{-N}$) is a typical pollutant that contributes to eutrophication in natural water bodies and presents a risk to aquatic ecosystems [3]. In 2020, global ammonia production increased by 2.9 million tons, reaching a total supply of 185 million tons [4]. Besides wastewater from residential and agricultural sources, emissions of $\text{NH}_4^+\text{-N}$ from industrial activities must not be disregarded [5]. Typically, industries such as food processing, rubber processing, textile dyeing and printing, leather manufacturing, fertilizer production, and others, discharge high levels of $\text{NH}_4^+\text{-N}$ concentration into water [6]. As an illustration, in China, the "Second National Pollution Source Census Bulletin" released in June 2020 revealed that industrial wastewater in China discharged 44,500 tons of $\text{NH}_4^+\text{-N}$ in 2017 [7]. In general, governments worldwide have set strict environmental standards for $\text{NH}_4^+\text{-N}$ [8].

For example, the United States Environmental Protection Agency (U.S. EPA) recommends that in freshwater systems, acute one-hour exposures should not exceed 17 mg/L (pH = 7.0 and T = 20 °C) and also regulates the chronic exposures [9]. Facing the urgent challenges of global warming, it is crucial to seek methods for treating $\text{NH}_4^+\text{-N}$ in industrial wastewater that are efficient, cost-effective, and characterized by low energy consumption [10,11].

Currently, a variety of $\text{NH}_4^+\text{-N}$ removal technologies are available, including physical methods like air stripping, ion exchange, and adsorption; chemical methods such as chemical precipitation and breakpoint chlorination; and biological methods like nitrification, denitrification, partial nitrification, and anaerobic ammonium oxidation [12–15]. In comparison, the growing concern about climate change and water conservation has drawn significant attention from researchers to investigate the potential of microalgae for biological carbon fixation and wastewater treatment [16–18]. However, microalgae technology for industrial wastewater treatment is not yet fully developed, and there are still areas of concern that require further research. On one hand, while microalgae primarily utilize $\text{NH}_4^+\text{-N}$ as their nitrogen source, excessive concentrations have been observed to induce toxic effects, thereby inhibiting growth [19]. On the other hand, microalgae are susceptible to the effects of coexisting pollutants in industrial wastewater, which can inhibit their growth. For example, the presence of salt compounds in industrial wastewater can diminish algal activity due to high osmotic pressure, thus impacting the treatment efficacy for $\text{NH}_4^+\text{-N}$ [20,21]. While certain types of microalgae can tolerate fluctuations in salinity, exposure to salinity stress often leads to reduced biomass productivity, mainly due to the significant energy requirements for osmoregulation [22].

Oocystis lacustris, a member of the *Oocystis* genus, is commonly distributed across various water bodies, particularly thriving in freshwater ecosystems, where it dominates the planktonic community in small lakes and ponds [23]. Additionally, previous research has found that *Oocystis lacustris* can thrive in food waste digestate with high $\text{NH}_4^+\text{-N}$ concentrations, and researchers have identified it as one of the prevalent algae species in surface water with elevated salinity levels [24]. As such, *Oocystis lacustris* holds promising potential for the treatment of saline $\text{NH}_4^+\text{-N}$ wastewater. Nonetheless, it is essential to conduct laboratory experiments to evaluate the toxicity of $\text{NH}_4^+\text{-N}$ and to explore the tolerance of *Oocystis lacustris* to saline industrial wastewater, as well as assess its effectiveness in removing $\text{NH}_4^+\text{-N}$.

Therefore, with the goal of further advancing the application of microalgae technologies in industrial wastewater treatment, this study simulated the characteristics of saline $\text{NH}_4^+\text{-N}$ wastewater and investigated the growth of *Oocystis lacustris* in the wastewater, as well as its efficiency in removing $\text{NH}_4^+\text{-N}$. Importantly, this research analyzed the physiological status, lipid accumulation, key enzyme activity, and changes in the antioxidant system of *Oocystis lacustris* during the treatment of saline $\text{NH}_4^+\text{-N}$ wastewater, contributing to a more comprehensive understanding of microalgae-based saline $\text{NH}_4^+\text{-N}$ wastewater treatment technology. Furthermore, the potential mechanisms involved in the removal of $\text{NH}_4^+\text{-N}$ have been examined, aiming to provide valuable guidelines for the treatment of saline $\text{NH}_4^+\text{-N}$ wastewater using microalgae.

2. Materials and Methods

2.1. Instruments and Reagents

The experimental devices used in this study included an intelligent light incubator (GXZ, Ningbo Jiangnan Instrument Factory, Ningbo, China), algal cell counter (IA1000, Shanghai Ruiyu Biotechnology Co., Ltd., Shanghai, China), spectral color illuminometer (OHSP-350P, Hangzhou Hopoo Light & Color Technology Co., Ltd., Hangzhou, China), UV-visible spectrophotometer (UV-1900, Shimadzu, Kyoto, Japan), vertical pressure steam sterilizer (LDZM-40KCS, Shanghai Shenan Medical Equipment Factory, Shanghai, China), UV sterilization bench (VD-850, Shanghai Dingke Scientific Instrument Co., Ltd., Shanghai, China), Heraeus Multifuge X1 refrigerated centrifuge (Thermo Fisher Scientific, Waltham,

MA, USA), and ultrasonic cell disruptor (JY92-II, Ningbo Xinzhi Biotechnology Co., Ltd., Ningbo, China).

The reagents used in this study, including sodium sulfate (Na_2SO_4) and phosphate-buffered saline (PBS) purchased from Shanghai Aladdin Biochemical Technology Co., Ltd. (Shanghai, China), and ammonium sulfate $[(\text{NH}_4)_2\text{SO}_4]$ obtained from China National Pharmaceutical Group Corporation (Beijing, China), were all of analytical grade. Additionally, a BG11 medium was used which contained the following components: NaNO_3 (1.5 g/L); $\text{K}_2\text{HPO}_4 \cdot 3\text{H}_2\text{O}$ (40 mg/L); $\text{MgSO}_4 \cdot 7\text{H}_2\text{O}$ (75 mg/L); $\text{CaCl}_2 \cdot 2\text{H}_2\text{O}$ (36 mg/L); Na_2CO_3 (20 mg/L); $\text{FeCl}_3 \cdot 6\text{H}_2\text{O}$ (3.15 mg/L); citric acid (6 mg/L); and 1 mL of microelements composed of H_3BO_3 (2.86 mg/L), $\text{MnCl}_2 \cdot 4\text{H}_2\text{O}$ (1.81 mg/L), $\text{ZnSO}_4 \cdot 7\text{H}_2\text{O}$ (0.22 mg/L), $\text{Na}_2\text{MoO}_4 \cdot 2\text{H}_2\text{O}$ (0.39 mg/L), $\text{CuSO}_4 \cdot 5\text{H}_2\text{O}$ (0.08 mg/L), and $\text{Co}(\text{NO}_3)_2 \cdot 6\text{H}_2\text{O}$ (0.05 mg/L) in 1000 mL, and the pH was adjusted to 7.1 using 0.1 mol/L HCl and 0.1 mol/L NaOH.

2.2. Algal Strain and Culture Conditions

The algal strain, *Oocystis lacustris* (FACHB-2069), used in this study was obtained from the Freshwater Algal Culture Collection at the Institute of Hydrobiology, Chinese Academy of Sciences (Wuhan, China). The propagation of the strain involved the preparation and sterilization of the BG11 medium through autoclaving at 100 kPa and 121 °C for 20 min. The algal inoculum was introduced into the culture medium at a volume ratio of 1:5, and the resulting mixture was then placed in an intelligent light incubator. They were maintained at 25 ± 1 °C and illuminated by 60 $\mu\text{mol photons m}^{-2} \text{s}^{-1}$ from daylight-type fluorescent lamps using a light:dark photoperiod of 12:12. Irradiance was measured by a spectral color illuminometer. The conical flasks were manually agitated three times daily at regular intervals to prevent algal cell sedimentation.

2.3. The Effect of High Concentrations of Na_2SO_4 on Algal Growth

Na_2SO_4 is a common dyeing accelerant for reactive dyes, favored for its superior performance over NaCl [25]. The concentration of SO_4^{2-} in dyeing wastewater typically ranges from 200 to 5000 mg/L, sometimes exceeding 10,000 mg/L [25,26]. Generally, wastewater is considered “high-salinity” when the concentration of inorganic salts ranges from 1 to 3.5% w/w. Therefore, this study investigated the effects of Na_2SO_4 concentrations ranging from 5 to 20 g/L (equivalent to approximately 3380 to 13,520 mg/L of SO_4^{2-}) on microalgal growth. Accordingly, the BG11 medium (the conductivity was 0.19 S/m) was prepared using Na_2SO_4 as an inorganic salt source at concentrations of 5, 10, 15, and 20 g/L (the conductivities were 0.78 S/m, 1.22 S/m, 1.64 S/m, and 2.07 S/m), respectively. The algal cultures in the exponential growth phase (on the 4th to 6th day after inoculation) were utilized. Considering the requirements for the hydraulic retention time (HRT) and treatment efficiency in the wastewater treatment, the initial concentration of microalgae was established at 8×10^5 cells/L, surpassing the standards outlined by the OECD (2011) Test No. 201 and other pertinent guidelines for algal growth inhibition tests [27]. A control group using the standard BG11 medium was established for comparative analysis. During the tests, a 50 mL microalgal suspension was cultured in a 100 mL conical flask sealed with a breathable sealing film. The cultivation conditions for *Oocystis lacustris*, including illumination, temperature, and agitation, were consistent with the methods described in Section 2.2 regarding the cultivation of algal strains. This experimental section was conducted three times to ensure the reproducibility of the results. All tests included triplicates of each Na_2SO_4 concentration and five replicates of the control sample. The samples were taken every 24 h to measure the algal cell density (Section 2.5.1).

2.4. NH_4^+ -N Removal by *Oocystis lacustris* in Simulated Saline Wastewater

In the textile printing and dyeing process, printing necessitates the utilization of significant quantities of urea, which undergoes transformation into NH_4^+ -N during the biological treatment of wastewater. Additionally, the post-finishing treatment of cotton fabrics frequently entails the application of liquid ammonia to enhance their sheen and

durability, thereby directly contributing to the generation of $\text{NH}_4^+\text{-N}$ [26]. The concentration of $\text{NH}_4^+\text{-N}$ in textile printing and dyeing wastewater ranges from 0.5 to 75 mg/L [26]. Therefore, nitrogen components were removed from the BG11 medium, and the Na_2SO_4 concentration was set to 10 g/L. $\text{NH}_4^+\text{-N}$ concentrations of 1, 5, 10, 30, and 50 mg/L were then prepared to simulate saline $\text{NH}_4^+\text{-N}$ wastewater in our study. The BG11 medium containing 10 g/L Na_2SO_4 served as the control group. *Oocystis lacustris* cultures in the exponential growth phase were inoculated into the simulated wastewater at an initial cell density of 8×10^5 cells/mL, referred to as the EX phase *Oocystis lacustris* treatment group. To investigate the effect of *Oocystis lacustris* during stationary growth phases (on the 8th to 10th day after inoculation) on $\text{NH}_4^+\text{-N}$ removal, the microalgae in the stationary growth phase were inoculated into the simulated wastewater at an initial cell density of 2×10^7 cells/mL. This group was referred to as the STA phase *Oocystis lacustris* treatment group. The cultivation conditions, including illumination, temperature, and agitation, remained consistent with the methods outlined in Section 2.2. This experimental section was also repeated three times to ensure result reproducibility. Each test included triplicates of each $\text{NH}_4^+\text{-N}$ concentration and five replicates of the control sample. Given that enzyme assays require a larger quantity of algal cells, an additional three replicates were added to the treatment groups that needed enzyme activity measurement. The samples were collected at fixed intervals to measure algal cell density (Section 2.5.1), $\text{NH}_4^+\text{-N}$ concentration (Section 2.5.2), and physiological parameters (Section 2.5.3). Additionally, under the conditions of pH = 7.1 and the temperature = 25 °C, the proportion of NH_4^+ unionized as NH_3 was less than 1%.

2.5. Analytical Methods

2.5.1. Algal Cell Density

First, 1 mL of a microalgal solution was mixed with 10 μL of Lugol's solution for fixation. Subsequently, 30 μL of the mixture was transferred to a cell counting chamber, and the algal cell density was measured using the Countstar algal cell counter. During the counting process, each sample was measured three times for replicability. The percent inhibition in yield ($\%I_y$) was calculated for each treatment replicate as follows [27]:

$$\%I_y = \frac{(Y_c - Y_T)}{Y_c} \times 100 \quad (1)$$

where $\%I_y$ represents the percent inhibition of yield, Y_c represents the mean value for yield in the control group, and Y_T represents the value for yield for the treatment replicate. The yield is calculated as the biomass at the end of the test minus the starting biomass for each single vessel of controls and treatments.

2.5.2. $\text{NH}_4^+\text{-N}$ Concentrations

$\text{NH}_4^+\text{-N}$ concentrations were determined via Nessler's reagent method, with each sample being measured three times to ensure reproducibility [28].

2.5.3. Physiological Parameters of the Microalgae

For the determination of chlorophyll-a (*Chl-a*), the alga sample (10 mL) was collected by centrifugation with 10,000 rpm for 10 min. The collected algal cells were frozen and thawed four times in the dark. Next, the solids were steeped in an acetone 80% solution at 4 °C for 24 h. At last, the acetone solution containing chlorophyll-a was centrifuged again with 10,000 rpm for 10 min and the supernatant was measured by a UV-visible spectrophotometer with OD_{630} , OD_{647} , OD_{664} , and OD_{750} [29,30].

$$\text{Chl} - a = \frac{11.5(\text{OD}_{664} - \text{OD}_{750}) - 1.54(\text{OD}_{647} - \text{OD}_{750}) - 0.08(\text{OD}_{630} - \text{OD}_{750})V_1}{V} \quad (2)$$

where *Chl-a* is the chlorophyll-a concentration of the sample (mg/L), V_1 is the volume of the sample after extraction (mL), and V is the volume of the sample (mL).

To investigate soluble protein, superoxide dismutase (SOD), catalase (CAT), malondialdehyde (MDA), triglycerides (TAG), nitrate reductase (NR), and glutamine synthetase (GS) within microalgae, algal cells were disrupted first. Algal cells were collected from the microalga suspension (40 mL) by centrifugation (10,000 rpm) at 4 °C for 10 min. The cell pellets were washed by pre-cooled phosphate-buffered saline (PBS) solution (50 mmol/L, pH 7.0) twice and re-suspended in 6 mL of a PBS solution. Cell homogenization was conducted by ultrasonic cell disintegration at 650 W for 25 cycles (ultrasonic time: 3 s; rest time: 9 s) in an ice bath. The disrupted cells were then centrifuged at 10,000 rpm for 10 min at 4 °C, and the supernatant was collected and kept on ice for soluble protein content, MDA content, TAG content, and enzymes activity measurements.

The assay kits for measuring soluble protein (product no. QYS-237014), SOD (product no. QYS-23028), CAT (product no. QYS-23030), MDA (product no. QYS-23036), TAG (product no. QYS-234006), NR (product no. QYS-232003), and GS (product no. QYS-232017), were purchased from Qiyi Biological technology (Shanghai) Co., Ltd. (Shanghai, China). Soluble protein content was determined using the bicinchoninic acid (BCA) method at 562 nm wavelength using a UV-visible spectrophotometer. SOD activity was evaluated utilizing the nitro-blue tetrazolium dye (NBT) method at a 560 nm wavelength using a UV-visible spectrophotometer. CAT activity was assessed based on H₂O₂ decomposition, measured at 240 nm with a UV-visible spectrophotometer. The MDA level was determined by the formation of the MDA-TBA adduct formed by the reaction of MDA and thiobarbituric acid (TBA) under high temperature (90–100 °C), with absorbance measured at 535 nm using a UV-visible spectrophotometer. These enzyme activities and the MDA content were quantified by protein concentration. The enzyme activity unit (U) was defined as the amount of enzyme required to catalyze 1 μmol of substrate per minute. The TAG content was determined using a UV-visible spectrophotometer at 420 nm. The colorimetric principle was as follows: TAG was saponified by KOH to hydrolyze into glycerol and fatty acids. Glycerol was oxidized to formaldehyde by periodic acid. In the presence of chloride ions, formaldehyde condensed with acetone to produce a yellow substance. The NR activity was determined by monitoring the oxidation of NADH at 340 nm (UV-visible spectrum), dependent on the reduction of NO₃⁻ to NO₂⁻. The GS activity was determined by the reverse-glutamyl transferase reaction, which measured the formation of glutamyl hydroxamate using UV-visible spectrophotometer at 540 nm. One unit of enzymatic activity (U) was defined as the formation of 1 μmol of γ-glutamyl hydroxamate per min. These enzyme activities and TAG content were quantified by the algal cell concentration. The assays mentioned above were conducted following the user manual instructions of the assay kits, with each sample subjected to triplicate measurements.

2.5.4. Subcellular Structures of the Microalgae

The *Oocystis lacustris* cells were initially fixed in 3% glutaraldehyde in a 0.1 mol/L cacodylate buffer, followed by fixation in 1% aqueous osmium tetroxide in a 0.1 mol/L cacodylate buffer. After dehydration in acetone and embedding in Spurr's resin, ultrathin sections were prepared and stained with uranyl acetate and lead citrate [31]. The sections were then observed under a Hitachi HC-1 transmission electron microscope (TEM) at an accelerating voltage of 80 kV.

2.5.5. Data Processing and Analysis

Data analysis was conducted using the SPSS software statistical package (SPSS version 17.0 for Windows). The mean and standard error of the mean (S.E.M) were calculated for each parameter. The results were compared to determine the toxic effects by a one-way analysis of variance (ANOVA) and graphically presented using GraphPad Prism version 6 (GraphPad Software Inc., La Jolla, CA, USA). The significance level was set at *p*-value 0.05.

3. Results and Discussion

3.1. Influence of Different Na_2SO_4 Concentrations on the Growth of *Oocystis lacustris*

Figure 1 shows the growth of *Oocystis lacustris* at different concentrations of Na_2SO_4 . The cell concentration of *Oocystis lacustris* increased across all tested Na_2SO_4 concentrations, despite significant differences in the growth rates (Figure 1a). On the 7th day of cultivation, the cell concentration of *Oocystis lacustris* in the 20 g/L Na_2SO_4 group was only half that of the control group. The growth inhibition (Figure 1b) shows that the highest inhibition occurred on the 1st day of cultivation under saline conditions, likely due to the significant impact of Na_2SO_4 exposure on algal growth. On the 2nd day, there was partial relief in growth inhibition. However, except for the 5 g/L concentration, Na_2SO_4 continued to inhibit *Oocystis lacustris* growth, reaching a second peak of inhibition by the 5th day of cultivation. In addition to altering osmotic pressure, Na_2SO_4 may also compete with structurally similar nutrients for transport proteins, thereby reducing the ability of algal cells to acquire essential other nutrients for growth, such as selenite and molybdate ions [32–34]. It was also observed that as the algal cell concentration increased, the standard deviation among replicate samples widened. This could be attributed to counting errors caused by the aggregation of *Oocystis lacustris*. To ensure the reliability of observation, two additional replicate experiments were conducted, as depicted in Figures S1 and S2 in Supplementary Information. Although variations in numerical values existed in algal cell concentration between different experimental batches, the overall inhibitory trend remained consistent. Due to the results indicating that under treatment with 10 g/L Na_2SO_4 , although *Oocystis lacustris* exhibited significant growth inhibition, recovery was observed by the 7th day. Furthermore, the concentration of 10 g/L Na_2SO_4 closely resembles the characteristics of actual high-salinity wastewater. Subsequent experiments in our study were conducted using 10 g/L Na_2SO_4 to simulate saline wastewater.

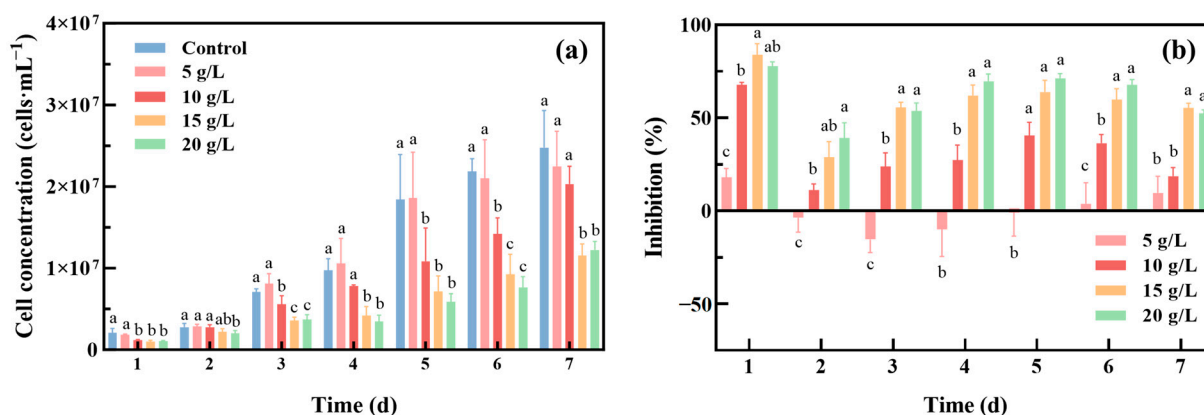


Figure 1. Growth of *Oocystis lacustris* at different Na_2SO_4 concentrations. (a) Cell concentration; (b) inhibition of yield. (At the same cultivation time, different letters on adjacent bars indicate significant differences ($p < 0.05$), while the same letter indicates no significant difference).

3.2. Effects of *Oocystis lacustris* on NH_4^+ -N Removal

Figure 2a shows the NH_4^+ -N removal efficiency of *Oocystis lacustris* with an initial cell density of 8×10^5 cells/mL (EX phase) at different concentrations of NH_4^+ -N. *Oocystis lacustris* exhibited high removal efficiencies at low concentrations of NH_4^+ -N, achieving almost 100% removal rate by the 2nd day for 1 mg/L NH_4^+ -N and by the 7th day for 5 mg/L NH_4^+ -N. However, as the NH_4^+ -N concentration exceeded 10 mg/L, the NH_4^+ -N removal efficiency by the algae decreased, reaching 70% on the 11th day. As the NH_4^+ -N concentration further increased to 30 mg/L, the removal efficiency of the algae remained low. This phenomenon was closely related to the growth state of algal cells (Figure 2b,c), which illustrated the growth of algal cells and the corresponding growth inhibition over time. During the 11-day growth period, the cell density of *Oocystis lacustris* in the control group

increased from 8×10^5 to 4.6×10^7 cells/mL. The presence of $\text{NH}_4^+\text{-N}$ obviously inhibited the growth of *Oocystis lacustris*. On the 11th day of the $\text{NH}_4^+\text{-N}$ treatment experiment, in the treatment groups with $\text{NH}_4^+\text{-N}$ concentrations ranging from 1 to 50 mg/L, the inhibition rate of microalgae ranged from 23.6% to 77.7%. When the $\text{NH}_4^+\text{-N}$ concentrations were 1 mg/L and 5 mg/L, although the removal rate of $\text{NH}_4^+\text{-N}$ could reach nearly 100%, the growth inhibition rate of *Oocystis lacustris* still ranged from 23.6% to 45.4%. The consistent phenomena observed from replicate experiments are illustrated in Figures S3 and S4. This suggests that *Oocystis lacustris* in the EX phase was sensitive to the $\text{NH}_4^+\text{-N}$ concentration in saline wastewater. Previous studies have indicated that high $\text{NH}_4^+\text{-N}$ levels mainly disrupt the normal transmembrane proton gradient from adenosine triphosphate (ATP) to ADP in algal chloroplasts, inhibiting photosynthesis. This disruption may occur through mechanisms such as damage to protein subunits in chloroplasts, thereby hindering the function of photosystem II (PSII) and inhibiting cell growth [35–37].

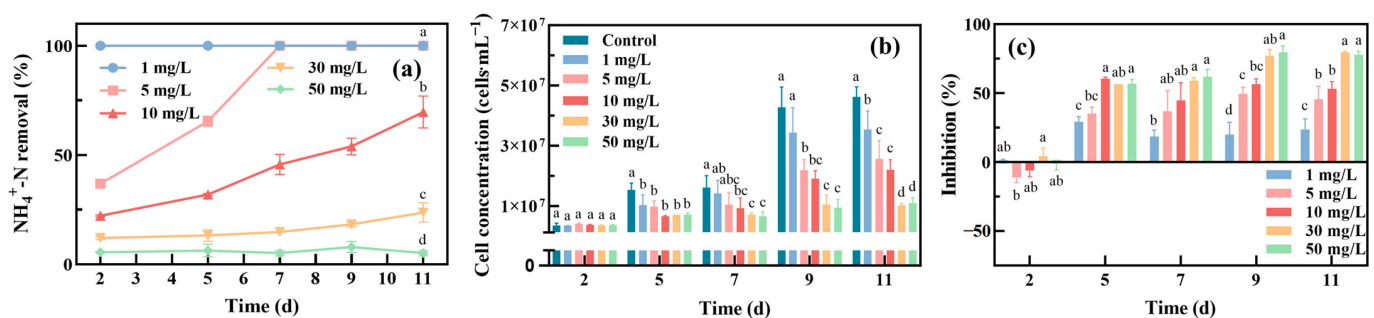


Figure 2. Treatment of *Oocystis lacustris* in the EX phase (8×10^5 cells/mL) with different concentrations of $\text{NH}_4^+\text{-N}$. (a) $\text{NH}_4^+\text{-N}$ removal rate; (b) cell concentration; (c) inhibition of yield. (At the same cultivation time, different letters on adjacent bars indicate significant differences ($p < 0.05$), while the same letter indicates no significant difference).

Figure 3a illustrates the $\text{NH}_4^+\text{-N}$ removal efficiency of *Oocystis lacustris* with an initial cell density of 2×10^7 cells/mL (STA phase) at different concentrations of $\text{NH}_4^+\text{-N}$. Compared with the EX phase, the $\text{NH}_4^+\text{-N}$ removal efficiency of *Oocystis lacustris* in the STA phase was improved. $\text{NH}_4^+\text{-N}$ concentrations of 1, 5, and 10 mg/L resulted in almost complete removal by *Oocystis lacustris* on the 1st, 2nd, and 4th days of treatment, respectively. As the $\text{NH}_4^+\text{-N}$ concentration increased to 30 and 50 mg/L, its removal efficiency remained low, with $\text{NH}_4^+\text{-N}$ removal rates of 35.2% and 16.2% on the 8th day of treatment, respectively. Additionally, compared to the growth phase of EX, *Oocystis lacustris* in the STA phase exhibited a slower rate of cell proliferation during $\text{NH}_4^+\text{-N}$ removal. By the 8th day of cultivation, the cell density of *Oocystis lacustris* in the control group had only increased 2.5-fold. The slower growth rate resulted in the peak inhibition of $\text{NH}_4^+\text{-N}$ occurring on the first day of cultivation. Subsequently, the growth inhibition remained stable, with the growth inhibition of algal cells in saline $\text{NH}_4^+\text{-N}$ environments all below 50%. The consistent observations from replicate experiments are depicted in Figures S5 and S6. It indicates that microalgae in the STA phase with high cell densities might be more advantageous for treating saline $\text{NH}_4^+\text{-N}$ wastewater. Despite initially experiencing some toxicity impact during treatment, the microalgae demonstrated rapid stabilization in growth. Moreover, they exhibited high efficiency in removing $\text{NH}_4^+\text{-N}$.

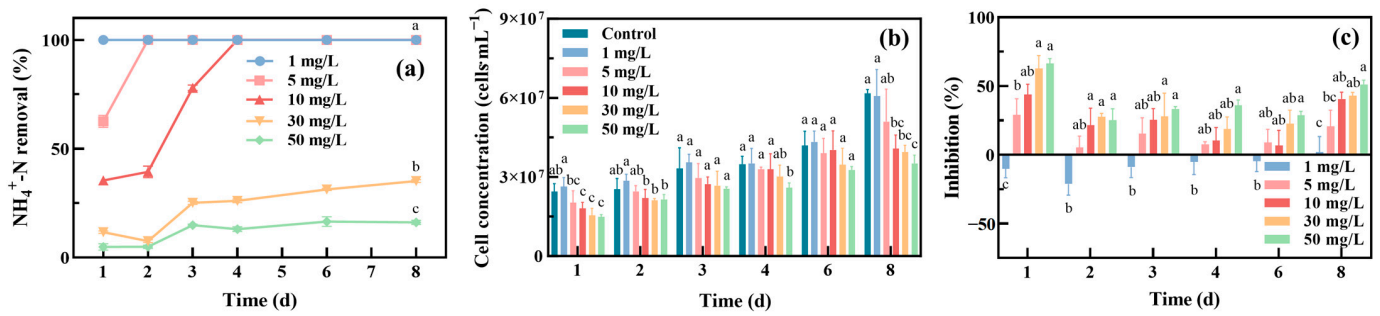


Figure 3. Treatment of *Oocystis lacustris* in the STA phase (2×10^7 cells/mL) with different concentrations of $\text{NH}_4^+\text{-N}$. (a) $\text{NH}_4^+\text{-N}$ removal rate; (b) cell concentration; (c) inhibition of yield. (At the same cultivation time, different letters on adjacent bars indicate significant differences ($p < 0.05$), while the same letter indicates no significant difference).

Table 1 displays the $\text{NH}_4^+\text{-N}$ removal efficiency achieved by typical microalgae. Given the diversity in species, culture conditions, and wastewater compositions, the $\text{NH}_4^+\text{-N}$ removal efficiency varies widely, ranging from 31% to over 97%. Such variability poses significant challenges for microalga-based wastewater treatment, particularly when handling large wastewater volumes. Moreover, there is a scarcity of studies examining $\text{NH}_4^+\text{-N}$ removal efficiency under high-salinity conditions. Therefore, this study aimed to investigate the $\text{NH}_4^+\text{-N}$ removal efficiency of *Oocystis lacustris* under high concentrations of Na_2SO_4 . While the removal efficiency may appear lower compared to the reported algal strains such as *Chlorella* sp., *Chlorococcum* sp., *Parachlorella kessleri*, and others, we explored the stress induced by high concentrations of Na_2SO_4 . To delve deeper into the physiological responses of *Oocystis lacustris* to saline $\text{NH}_4^+\text{-N}$ wastewater treatment, subsequent sections will undertake analyses of chlorophyll-a content, oxidative stress indicators, key nitrogen metabolism enzymes, and microscopic observations of algal cells. These investigations aim to lay a foundation for the potential application of *Oocystis lacustris* in treating saline $\text{NH}_4^+\text{-N}$ wastewater.

Table 1. The comparison of $\text{NH}_4^+\text{-N}$ treatment efficiency by typical microalgae.

Algal Strain	Initial $\text{NH}_4^+\text{-N}$ Concentration (mg/L)	$\text{NH}_4^+\text{-N}$ Removal Efficiency (%)	Salt Concentration	Wastewater	Ref.
<i>Chlorella</i> sp.	85.9 ± 1.1	93.9	/	Municipal wastewater	[38]
<i>Chlorella vulgaris</i>		85.30			
<i>Chlorococcum</i> sp. GD		91.72			
<i>Parachlorella kessleri</i> TY	80	92.68	$\text{NaCl} = 64 \text{ mg/L}$	Synthetic wastewater	[39]
<i>Scenedesmus obliquus</i>		93.04			
<i>Scenedesmus quadricauda</i>		97.03			
<i>Chlorella vulgaris</i>	10	53.12	/	Modified Bristol medium	[40]
<i>Scenedesmus</i> sp. LX1	15	31.1	/	Synthetic wastewater	[41]
<i>Scenedesmus quadricauda</i>	42~46	65	/	Synthetic sewage	[42]
<i>Chlorella</i> sp.	160	50.60	/	Mixed wastewater	[43]
<i>Oocystis lacustris</i>	1~50	15.2~99	$\text{Na}_2\text{SO}_4 = 10 \text{ g/L}$	Modified BG11 medium	This work

3.3. Variations in Chlorophyll-a and Soluble Protein Contents of *Oocystis lacustris*

Figure 4 illustrates the changes in chlorophyll-a and soluble protein contents in *Oocystis lacustris* cells treated with $\text{NH}_4^+\text{-N}$ on the 8th day with the presence of 10 g/L Na_2SO_4 . In the EX phase group of microalgae, when the $\text{NH}_4^+\text{-N}$ concentration exceeded 10 mg/L, there was a significant decrease in chlorophyll-a content, reaching only one-fifth of the level observed in the control group as the $\text{NH}_4^+\text{-N}$ concentration reached 30 mg/L (Figure 4a). The treatment group with $\text{NH}_4^+\text{-N}$ concentration at 5 mg/L was an outlier. As evident from the results of the two additional repeated experiments (Figures S7 and S8), at this concentration, the effect of $\text{NH}_4^+\text{-N}$ on chlorophyll-a content was not significant. Changes

in the soluble protein content of *Oocystis lacustris* cells were consistent with those of chlorophyll-a (Figure 4b). On the 8th day of treatment with 30 and 50 mg/L $\text{NH}_4^+\text{-N}$, the soluble protein content in the algal cells significantly decreased, reaching only 36% of the level observed in the control group. These reductions may be attributed to the detrimental effects of high $\text{NH}_4^+\text{-N}$ concentrations on the oxygen-evolving complex (OEC) of algal cells, leading to reduced OEC activity. Additionally, $\text{NH}_4^+\text{-N}$ diffusion within cells altered the pH of the thylakoid lumen, resulting in decreased ATP levels, thereby affecting chlorophyll-a synthesis [44,45].

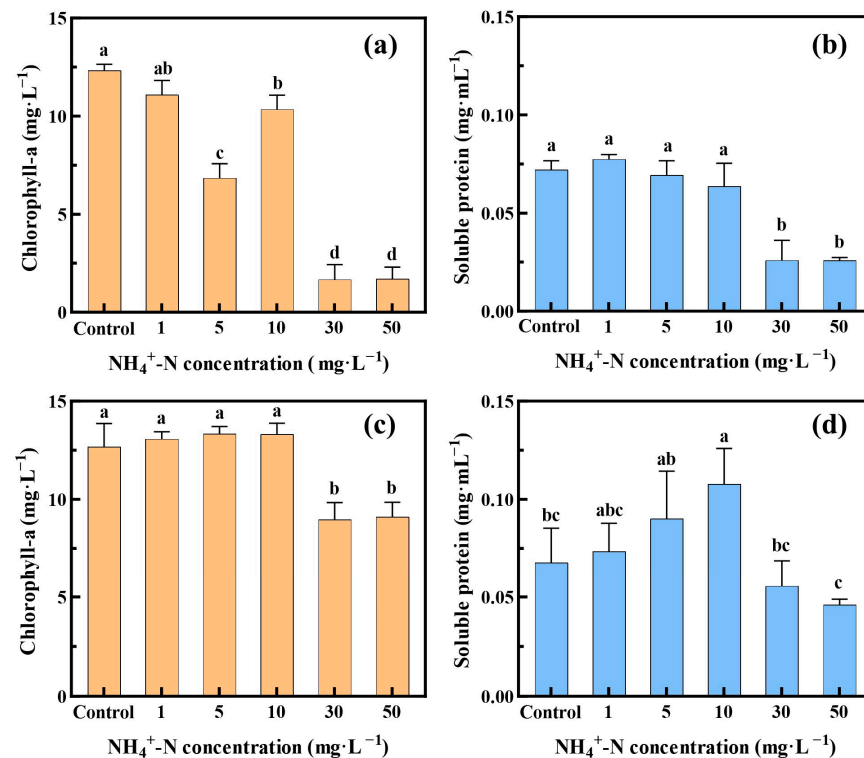


Figure 4. Variations in chlorophyll-a and soluble protein contents within *Oocystis lacustris* cells at different $\text{NH}_4^+\text{-N}$ concentrations on the 8th day. (a,b) Changes in chlorophyll-a and soluble protein contents within algal cells in the EX phase; (c,d) changes in chlorophyll-a and soluble protein contents within algal cells in the STA phase. (Different letters on adjacent bars indicate significant differences ($p < 0.05$), while the same letter indicates no significant difference).

In comparison, *Oocystis lacustris* in the STA phase exhibited stronger resistance to the toxic impacts of saline $\text{NH}_4^+\text{-N}$ wastewater. As the $\text{NH}_4^+\text{-N}$ concentration exceeded 30 mg/L, there was only a 29.3% decrease in chlorophyll-a content. On the other hand, with an increasing $\text{NH}_4^+\text{-N}$ concentration, the soluble protein content in the algal cells peaked at 0.108 mg/mL in the 10 mg/L $\text{NH}_4^+\text{-N}$ treatment group (Figure 4d). Subsequently, the soluble protein content gradually decreased, reaching a minimum of 0.046 mg/mL in the 50 mg/L $\text{NH}_4^+\text{-N}$ group. Research reports have indicated that the accumulation of soluble proteins in microalgae can enhance cell water retention capacity and protect vital compounds within the cell membrane [46,47]. Therefore, at lower concentrations of $\text{NH}_4^+\text{-N}$, the synthesis of soluble proteins in algal cells increased, whereas exposure to high concentrations of $\text{NH}_4^+\text{-N}$ inhibited and significantly damaged the synthesis of soluble proteins in algal cells.

3.4. Oxidative Stress Status of *Oocystis lacustris*

The oxidative stress induced by $\text{NH}_4^+\text{-N}$ and Na_2SO_4 may affect the growth status of *Oocystis lacustris* and the efficiency of $\text{NH}_4^+\text{-N}$ removal. MDA, a product of lipid peroxidation, is generally considered a primary biomarker for assessing oxidative stress

intensity [48–50]. Figure 5a,d shows the accumulation of MDA in algal cells during the removal of $\text{NH}_4^+\text{-N}$. For the microalgae in the EX phase (Figure 5a), the MDA content in *Oocystis lacustris* cells remained relatively stable in the 10 mg/L $\text{NH}_4^+\text{-N}$ treatment group compared with the control group. However, at a high $\text{NH}_4^+\text{-N}$ concentration (50 mg/L), the MDA content rapidly increased, indicating strong oxidative stress and significant oxidative damage to algal cells [51,52]. At the same time, the MDA content of *Oocystis lacustris* in the STA phase remained relatively stable (Figure 5d). Figure 5b,c,e,f shows the response of the antioxidant system in *Oocystis lacustris* through the evaluation of the concentrations of SOD and CAT in algal cells. SOD was considered the primary enzyme in the antioxidant system. Moreover, SOD catalyzed the dismutation reaction of superoxide radicals into hydrogen peroxide and oxygen molecules, which were further decomposed into water and molecular oxygen by enzymes such as CAT [53–55]. In the EX phase (Figure 5b,c), microalgae showed increased SOD and CAT activities with rising $\text{NH}_4^+\text{-N}$ concentrations. By the 8th day of treatment with 50 mg/L $\text{NH}_4^+\text{-N}$, the SOD activity doubled, while the CAT activity increased nearly fourfold compared to the control group. These changes, along with the replicated experimental results (Figures S9 and S10), indicate that during the EX phase, *Oocystis lacustris* was highly sensitive to the toxic effects of $\text{NH}_4^+\text{-N}$, leading to significant oxidative stress. In contrast, SOD and CAT activities within *Oocystis lacustris* cells during the STA phase showed only slight increases, even in the presence of 50 mg/L $\text{NH}_4^+\text{-N}$, suggesting slight oxidative stress.

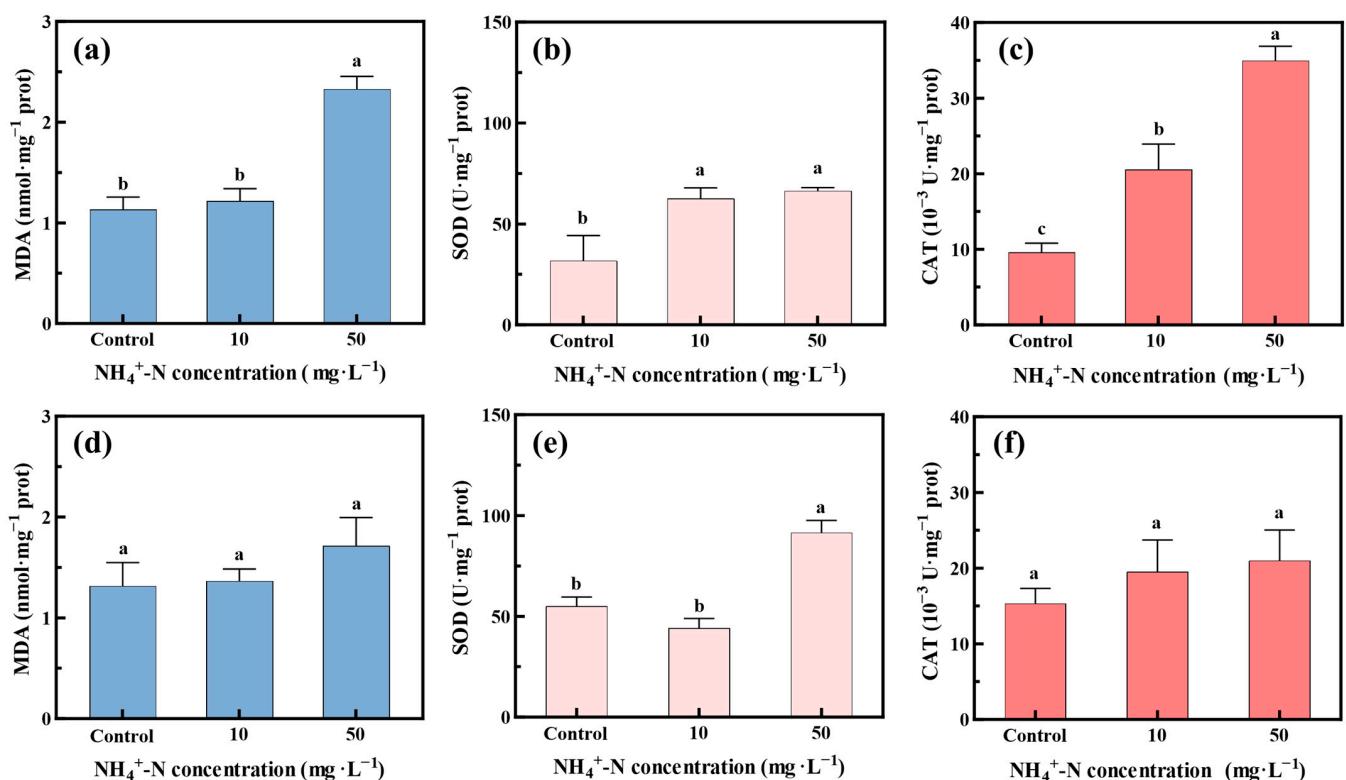


Figure 5. Oxidative stress status within *Oocystis lacustris* cells treated with different concentrations of $\text{NH}_4^+\text{-N}$ on the 8th day. (a–c) MDA concentration and SOD and CAT activities within algal cells in the EX phase; (d–f) MDA concentration and SOD and CAT activities within algal cells in the STA phase. (Different letters on adjacent bars indicate significant differences ($p < 0.05$), while the same letter indicates no significant difference).

3.5. Subcellular Structures of *Oocystis lacustris*

Figure 6 shows the cell morphology of *Oocystis lacustris* in the EX phase. In the control group, algal cells exhibited an elliptical or circular shape, with multiple layers of cell walls and well-organized chloroplasts. In each algal cell, there is a single pyrenoid enclosed by a

homogeneous matrix and surrounded by a thick starch sheath. When treated with 10 mg/L $\text{NH}_4^+\text{-N}$, the number of starch granules in the algal cells decreased (Figure 6b1–b3). This reduction may be attributed to the high metabolic state induced by $\text{NH}_4^+\text{-N}$ absorption with the presence of Na_2SO_4 , leading to the degradation and depletion of starch granules. When exposed to 50 mg/L $\text{NH}_4^+\text{-N}$ (Figure 6c1–c3), the starch sheath thickness in algal cells visibly decreased, with widened channels. Moreover, chloroplasts displayed overlapping arrangements instead of being organized in parallel, indicating possible chloroplast damage. Figure 7 shows the cell morphology of *Oocystis lacustris* in the STA phase. In both the control group and the 10 mg/L $\text{NH}_4^+\text{-N}$ treatment group, the main organelles of algal cells did not undergo visible changes. But similar to the algal cell in the EX phase, the number of starch grains decreased in the presence of $\text{NH}_4^+\text{-N}$. Additionally, a key morphological feature observed was the presence of some cells enveloped in a pectinaceous gelatinous sheath during growth. Sometimes, multiple algal cells aggregated into colonies, encased within a gelatinous sheath (Figure S11) [56,57]. When exposed to 50 mg/L $\text{NH}_4^+\text{-N}$, the gelatinous sheath ruptured, potentially increasing the susceptibility of the algal cells to external disruptions. This phenomenon indirectly indicates why *Oocystis lacustris* in the STA phase exhibits greater resistance to saline $\text{NH}_4^+\text{-N}$ stress.

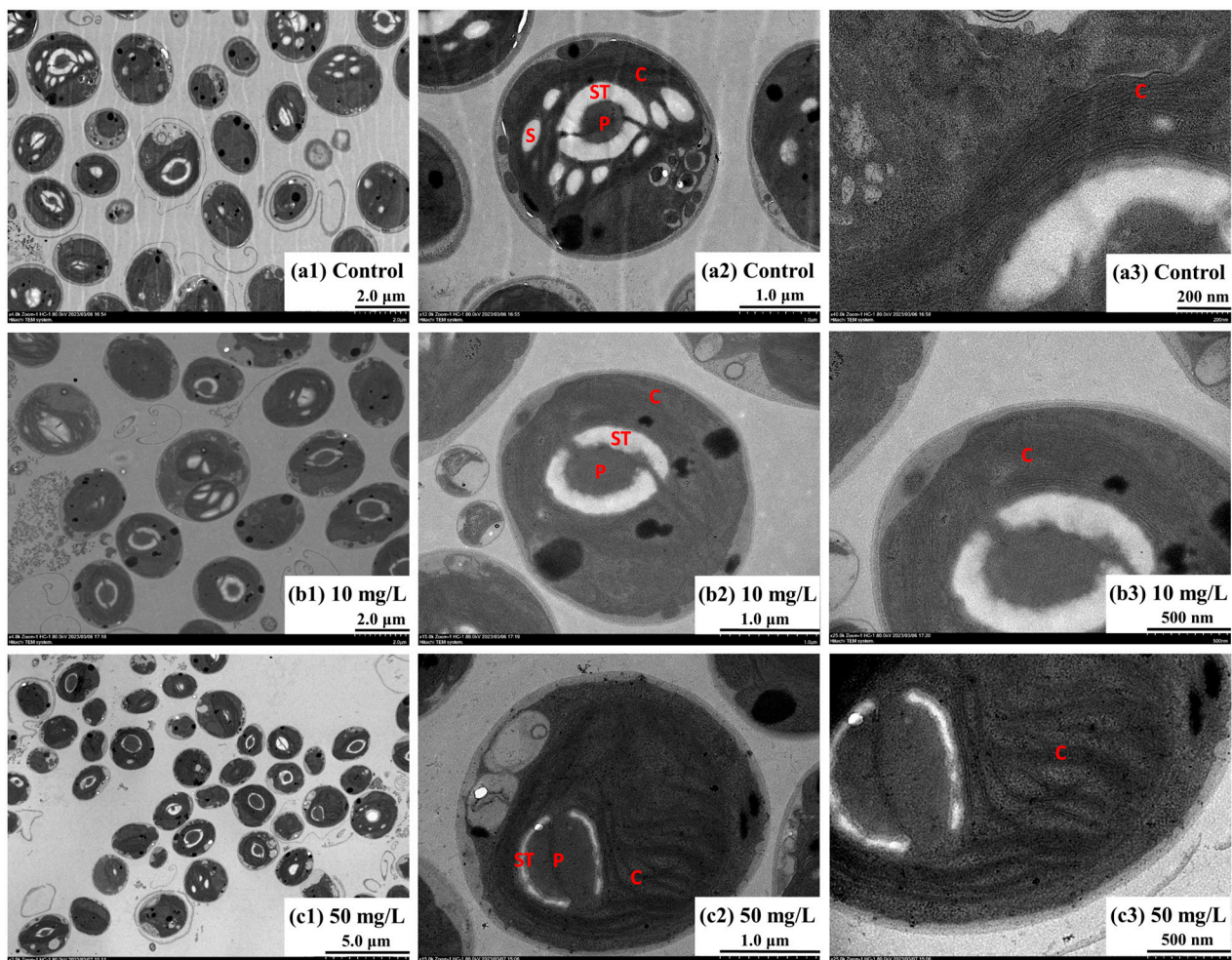


Figure 6. Microscopic morphology of *Oocystis lacustris* cells in the EX phase on the 8th day. (a1–a3) Control group; (b1–b3) 10 mg/L $\text{NH}_4^+\text{-N}$ treatment group; (c1–c3) 50 mg/L $\text{NH}_4^+\text{-N}$ treatment group. (C: chloroplast; ST: starch sheath; P: pyrenoid; S: starch grains).

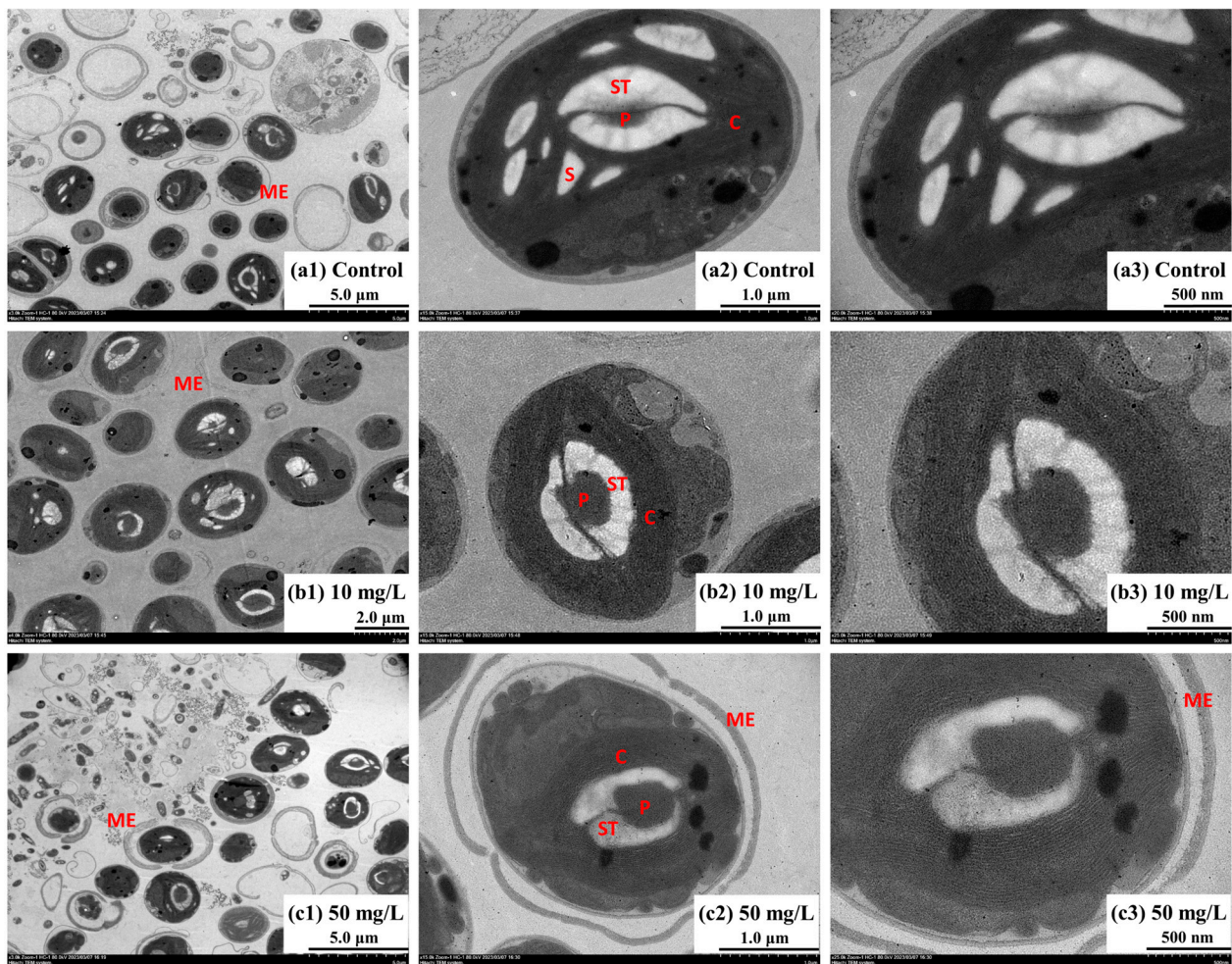


Figure 7. Microscopic morphology of *Oocystis lacustris* cells in the STA phase on the 8th day. (a1–a3) Control group; (b1–b3) 10 mg/L NH_4^+ -N treatment group; (c1–c3) 50 mg/L NH_4^+ -N treatment group. (C: chloroplast; ST: starch sheath; P: pyrenoid; S: starch grains; ME: mucilage envelope).

3.6. Removal Mechanism and Limiting Factors of *Oocystis lacustris* for NH_4^+ -N

Microalgae mainly utilized NH_4^+ -N by synthesizing glutamine from two molecules of α -ketoglutarate using GS-glutamate synthase (GS-GOGAT). The synthesized glutamine was then assimilated into amino acids, which were transported to various organelles for protein synthesis, nucleic acid synthesis, and other life activities. In NO_3^- -N utilization, microalgae initially reduced NO_3^- -N to NO_2^- -N using NR. NO_2^- -N was then transferred to the chloroplast and reduced to NH_4^+ -N using nitrite reductase. Compared to NO_3^- -N and NO_2^- -N, microalgae tend to preferentially utilize NH_4^+ -N directly, but NH_4^+ -N serves both as an essential nutrient and a toxic compound for microalgae. Li found that the GS activity increased with low concentrations of NH_4^+ -N but decreased as the NH_4^+ -N concentration increased [58]. This result aligns with our research findings (Figure 8a), showing an increase in GS activity when *Oocystis lacustris* in the EX phase was treated with 10 mg/L NH_4^+ -N, but a significant decrease when treated with 50 mg/L NH_4^+ -N. However, *Oocystis lacustris* in the STA phase exhibited no significant fluctuations in GS activity upon treatment with NH_4^+ -N, indicating minimal disruption to its GS-GOGAT pathway. In addition to the GS-GOGAT pathway, microalgae might also utilize NH_4^+ -N through the glutamate dehydrogenase (GDH) pathway. Tian et al. found that increasing NH_4^+ -N concentration, GS activity decreased while GDH expression levels increased [59]. In this pathway, α -ketoglutarate was converted to glutamate salt by GDH [60,61].

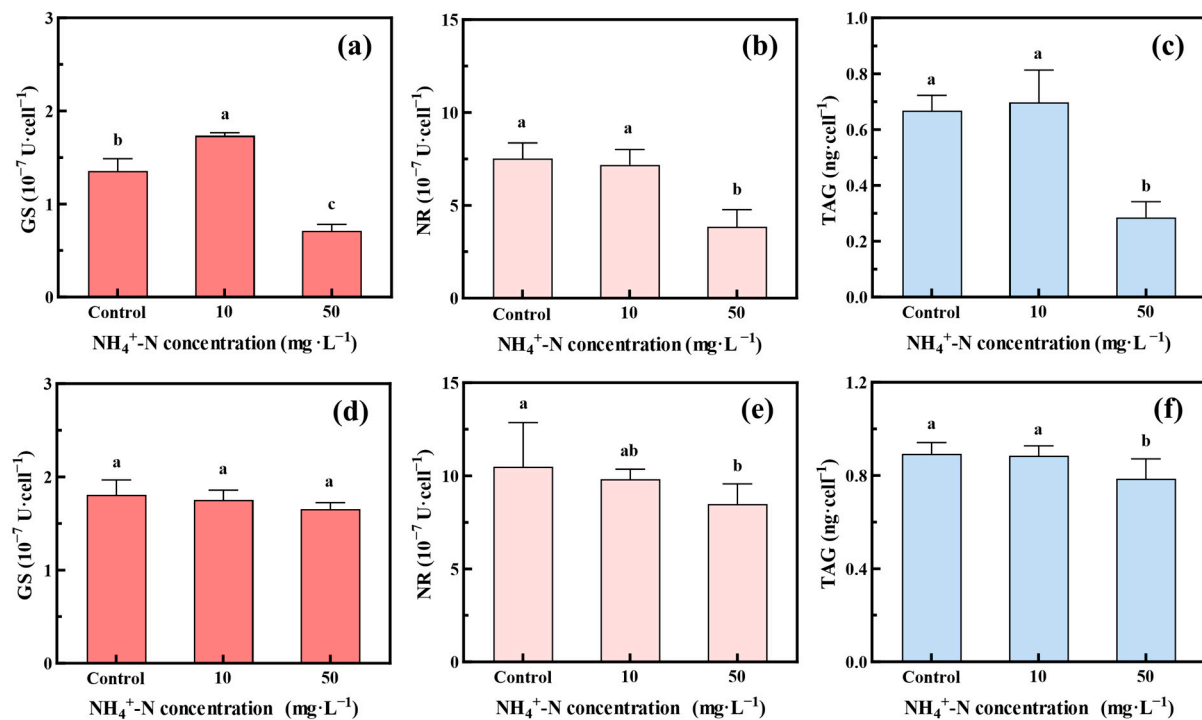


Figure 8. Changes in nitrogen metabolism enzymes and TAG activity within *Oocystis lacustris* treated by different $\text{NH}_4^+\text{-N}$ concentrations on the 8th day: (a) GS, (b) NR, and (c) TAG within algal cells in the EX phase; (d) GS, (e) NR, and (f) TAG within algal cells in the STA phase. (Different letters on adjacent bars indicate significant differences ($p < 0.05$), while the same letter indicates no significant difference).

Additionally, this study investigated alterations in NR activity during the $\text{NH}_4^+\text{-N}$ removal process. Both *Oocystis lacustris* in the EX and STA phases exhibited decreased NR activity when treated with $\text{NH}_4^+\text{-N}$. Compared to the control group, NR activity in algal cells subjected to 50 mg/L $\text{NH}_4^+\text{-N}$ decreased by 48.9% and 19.0%, respectively (Figure 8b,e). These findings align with those of Tian et al., who observed a significant downregulation of nitrate transport proteins (NTR2 and NTR3) when $\text{NH}_4^+\text{-N}$ was utilized as a sole nitrogen source or in combination with $\text{NO}_3^-\text{-N}$, indicating the inhibition of nitrate transport protein synthesis by $\text{NH}_4^+\text{-N}$ [59].

Further, TAG is the energy molecule stored as oil droplets within cells, crucial for adapting to adverse environmental conditions and maintaining cell survival processes. The TAG content within *Oocystis lacustris* in the EX phase (Figure 8c) markedly decreased when the $\text{NH}_4^+\text{-N}$ concentration reached 50 mg/L. This decline can be attributed to the damage caused by the elevated $\text{NH}_4^+\text{-N}$ concentration to chloroplasts, resulting in disrupted TAG synthesis and diminished TAG content [62,63]. For the *Oocystis lacustris* in the STA phase, the influence on cellular TAG content was comparatively minimal (Figure 8f), suggesting a potentially heightened resistance capability.

In summary, combining the results of the replicated experiments (Figures S12 and S13), *Oocystis lacustris* cultured in simulated saline $\text{NH}_4^+\text{-N}$ wastewater exhibited greater stability during the STA phase and demonstrated enhanced resistance to $\text{NH}_4^+\text{-N}$ stress following stabilization.

Although $\text{NH}_4^+\text{-N}$ utilization was more direct than $\text{NO}_3^-\text{-N}$, high concentrations of $\text{NH}_4^+\text{-N}$ can exert toxic effects on algal cells. This induced oxidative stress in algal cells, leading to an imbalance in antioxidant systems and lipid damage. Additionally, high $\text{NH}_4^+\text{-N}$ concentrations could disrupt the OEC of the algal cells and affect chlorophyll-a synthesis, thereby influencing the photosynthetic system of the algal cell. Moreover, the exposure of algal cells to high $\text{NH}_4^+\text{-N}$ concentrations in saline wastewater could lead to lower activities of nitrogen metabolism enzymes such as GS and NR. When using *Oocystis lacustris* to treat

saline wastewater containing $\text{NH}_4^+\text{-N}$, it is important to monitor the stability of microalgae growth and avoid excessively high concentrations of $\text{NH}_4^+\text{-N}$.

4. Conclusions

This study highlights the impact of high concentrations of Na_2SO_4 on the growth of *Oocystis lacustris*, demonstrating its tolerance up to 5 g/L, with an observed alleviation of growth inhibition at concentrations of 10 g/L within a week. In the STA phase, *Oocystis lacustris* (2×10^7 cells/mL) exhibited relatively higher efficiency in $\text{NH}_4^+\text{-N}$ removal in the presence of 10 g/L Na_2SO_4 , achieving almost 100% removal rate for 10 mg/L $\text{NH}_4^+\text{-N}$ by the 4th day of treatment. Additionally, it displayed robust resistance to the toxic effects of saline $\text{NH}_4^+\text{-N}$ wastewater, with minimal disruption observed in photosynthesis, protein synthesis, and the antioxidant system. Unlike previous studies that have focused on microalgae for $\text{NH}_4^+\text{-N}$ wastewater treatment, this study specifically aimed to investigate the feasibility of utilizing *Oocystis lacustris* for treating $\text{NH}_4^+\text{-N}$ wastewater under high salinity conditions. These findings have the potential to broaden the horizons of research in microalga-based wastewater treatment technology and offer fresh perspectives for industrial wastewater treatment.

Supplementary Materials: The following supporting information can be downloaded at: <https://www.mdpi.com/article/10.3390/toxics12050353/s1>, Figure S1: Growth of *Oocystis lacustris* at different Na_2SO_4 concentrations—September 2022. (a) Cell concentration; (b) inhibition of yield. (At the same cultivation time, different letters on adjacent bars indicate significant differences ($p < 0.05$), while the same letter indicates no significant difference.); Figure S2: Growth of *Oocystis lacustris* at different Na_2SO_4 concentrations—November 2022. (a) Cell concentration; (b) inhibition of yield. (At the same cultivation time, different letters on adjacent bars indicate significant differences ($p < 0.05$), while the same letter indicates no significant difference.); Figure S3: Treatment of *Oocystis lacustris* in the EX phase (8×10^5 cells/mL) with different concentrations of $\text{NH}_4^+\text{-N}$ —September 2022. (a) $\text{NH}_4^+\text{-N}$ removal rate; (b) cell concentration; (c) inhibition of yield. (At the same cultivation time, different letters on adjacent bars indicate significant differences ($p < 0.05$), while the same letter indicates no significant difference.); Figure S4: Treatment of *Oocystis lacustris* in the EX phase (8×10^5 cells/mL) with different concentrations of $\text{NH}_4^+\text{-N}$ —November 2022. (a) $\text{NH}_4^+\text{-N}$ removal rate; (b) cell concentration; (c) inhibition of yield. (At the same cultivation time, different letters on adjacent bars indicate significant differences ($p < 0.05$), while the same letter indicates no significant difference.); Figure S5: Treatment of *Oocystis lacustris* in the STA phase (2×10^7 cells/mL) with different concentrations of $\text{NH}_4^+\text{-N}$ —September 2022. (a) $\text{NH}_4^+\text{-N}$ removal rate; (b) cell concentration; (c) inhibition of yield. (At the same cultivation time, different letters on adjacent bars indicate significant differences ($p < 0.05$), while the same letter indicates no significant difference.); Figure S6: Treatment of *Oocystis lacustris* in the STA phase (2×10^7 cells/mL) with different concentrations of $\text{NH}_4^+\text{-N}$ —November 2022. (a) $\text{NH}_4^+\text{-N}$ removal rate; (b) cell concentration; (c) inhibition of yield. (At the same cultivation time, different letters on adjacent bars indicate significant differences ($p < 0.05$), while the same letter indicates no significant difference.); Figure S7: Variations in chlorophyll-a and soluble protein contents within *Oocystis lacustris* cells at different $\text{NH}_4^+\text{-N}$ concentrations on the 8th day—September 2022. (a,b) Changes in chlorophyll-a and soluble protein contents within algal cells in the EX phase; (c,d) changes in chlorophyll-a and soluble protein contents within algal cells in the STA phase. (Different letters on adjacent bars indicate significant differences ($p < 0.05$), while the same letter indicates no significant difference.); Figure S8: Variations in chlorophyll-a and soluble protein contents within *Oocystis lacustris* cells at different $\text{NH}_4^+\text{-N}$ concentrations on the 8th day—November 2022. (a,b) Changes in chlorophyll-a and soluble protein contents within algal cells in the EX phase; (c,d) changes in chlorophyll-a and soluble protein contents within algal cells in the STA phase. (Different letters on adjacent bars indicate significant differences ($p < 0.05$), while the same letter indicates no significant difference.); Figure S9: Oxidative stress status within *Oocystis lacustris* cells treated with different concentrations of $\text{NH}_4^+\text{-N}$ on the 8th day - September 2022. (a–c) MDA concentration and SOD and CAT activities within algal cells in the EX phase; (d–f) MDA concentration and SOD and CAT activities within algal cells in the STA phase. (Different letters on adjacent bars indicate significant differences ($p < 0.05$), while the same letter indicates no significant difference.); Figure S10: Oxidative stress status within *Oocystis lacustris* cells treated with different concentrations

of $\text{NH}_4^+\text{-N}$ on the 8th day - November 2022. (a–c) MDA concentration and SOD and CAT activities within algal cells in the EX phase; (d–f) MDA concentration and SOD and CAT activities within algal cells in the STA phase. (Different letters on adjacent bars indicate significant differences ($p < 0.05$), while the same letter indicates no significant difference.); Figure S11: Microscopic morphology of *Oocystis lacustris* cells in the EX phase on the 8th day: Two cells enveloped in a pectinaceous gelatinous sheath of control group; Figure S12: Changes in nitrogen metabolism enzymes and TAG activity within *Oocystis lacustris* treated by different $\text{NH}_4^+\text{-N}$ concentrations—September 2022: (a) GS, (b) NR, and (c) TAG within algal cells in the EX phase; (d) GS, (e) NR, and (f) TAG within algal cells in the STA phase. (Different letters on adjacent bars indicate significant differences ($p < 0.05$), while the same letter indicates no significant difference.); Figure S13: Changes in nitrogen metabolism enzymes and TAG activity within *Oocystis lacustris* treated by different $\text{NH}_4^+\text{-N}$ concentrations—November 2022: (a) GS, (b) NR, and (c) TAG within algal cells in the EX phase; (d) GS, (e) NR, and (f) TAG within algal cells in the STA phase. (Different letters on adjacent bars indicate significant differences ($p < 0.05$), while the same letter indicates no significant difference.).

Author Contributions: Conceptualization, Y.Z. (Yuqi Zhu) and Y.Z. (Yili Zhang); methodology, C.S.; software, Y.Z. (Yuqi Zhu) and Y.Z. (Yili Zhang); validation, L.Z.; formal analysis, Y.Z. (Yuqi Zhu) and C.S.; investigation, L.Z.; resources, C.S.; data curation, Y.Z. (Yuqi Zhu) and H.C.; writing—original draft preparation, Y.Z. (Yuqi Zhu); writing—review and editing, L.Z. and C.S.; visualization, Y.Z. (Yuqi Zhu) and C.S.; supervision, L.Z. and C.S.; project administration, C.S. and H.C.; funding acquisition, C.S. and H.C. All authors have read and agreed to the published version of the manuscript.

Funding: This research was funded by the Natural Science Foundation of Shanghai (no. 21ZR1401500), Ningbo Public Welfare Program (no. 2023S204), and the Fundamental Research Funds for the Central Universities (no. 2232023G-11).

Institutional Review Board Statement: Not applicable.

Informed Consent Statement: Not applicable.

Data Availability Statement: Data are contained within the article.

Conflicts of Interest: The authors declare no conflicts of interest.

References

- Oliveira, M.; Machado, A. The role of phosphorus on eutrophication: A historical review and future perspectives. *Environ. Technol. Rev.* **2013**, *2*, 117–127. [[CrossRef](#)]
- Giri, S. Water quality prospective in Twenty First Century: Status of water quality in major river basins, contemporary strategies and impediments: A review. *Environ. Pollut.* **2021**, *271*, 116332. [[CrossRef](#)] [[PubMed](#)]
- Gardner, W.S.; Newell, S.E.; McCarthy, M.J.; Hoffman, D.K.; Lu, K.; Lavrentyev, P.J.; Hellweger, F.L.; Wilhelm, S.W.; Liu, Z.; Bruesewitz, D.A. Community biological ammonium demand: A conceptual model for cyanobacteria blooms in eutrophic lakes. *Environ. Sci. Technol.* **2017**, *51*, 7785–7793. [[CrossRef](#)]
- Association, I.F. *Public Summary Medium-Term Fertilizer Outlook 2021–2025*; International Fertilizer Association: Paris, France, 2021.
- Billen, G.; Garnier, J.; Deligne, C.; Billen, C. Estimates of early-industrial inputs of nutrients to river systems: Implication for coastal eutrophication. *Sci. Total Environ.* **1999**, *243*, 43–52. [[CrossRef](#)]
- Karri, R.R.; Sahu, J.N.; Chimmiri, V. Critical review of abatement of ammonia from wastewater. *J. Mol. Liq.* **2018**, *261*, 21–31. [[CrossRef](#)]
- Ministry of Ecology and Environment of the People's Republic of China. *The Second National Pollution Source Census Bulletin*; Ministry of Ecology and Environment of the People's Republic of China: Beijing, China, 2020.
- Environmental Laws and Regulation. TERI Information Digest on Energy and Environment. *Indian J.* **2022**, *21*, 200–201.
- USEPA. *Aquatic Life Ambient Water Quality Criteria for Ammonia-Freshwater 2013*; Office of Water; USEPA: Washington, DC, USA, 2013.
- Wu, Z.; Zhu, W.; Liu, Y.; Peng, P.; Li, X.; Zhou, X.; Xu, J. An integrated three-dimensional electrochemical system for efficient treatment of coking wastewater rich in ammonia nitrogen. *Chemosphere* **2020**, *246*, 125703. [[CrossRef](#)] [[PubMed](#)]
- Ye, M.; Li, Y.Y. Methanogenic treatment of dairy wastewater: A review of current obstacles and new technological perspectives. *Sci. Total Environ.* **2023**, *866*, 161447. [[CrossRef](#)]
- Zhang, Y.; Yu, Z.; Hu, Y.; Song, C.; Li, F.; He, W.; Wang, X.; Li, Z.; Lin, H. Immobilization of nitrifying bacteria in magnetic PVA-SA-diatomite carrier for efficient removal of $\text{NH}_4^+\text{-N}$ from effluents. *Environ. Technol. Innov.* **2021**, *22*, 101407. [[CrossRef](#)]
- Xiang, S.; Liu, Y.; Zhang, G.; Ruan, R.; Wang, Y.; Wu, X.; Zheng, H.; Zhang, Q.; Cao, L. New progress of ammonia recovery during ammonia nitrogen removal from various wastewaters. *World J. Microbiol. Biotechnol.* **2020**, *36*, 144.

14. Han, B.; Butterly, C.; Zhang, W.; He, J.z.; Chen, D. Adsorbent materials for ammonium and ammonia removal: A review. *J. Clean. Prod.* **2021**, *283*, 124611. [[CrossRef](#)]
15. Chai, W.S.; Chew, C.H.; Munawaroh, H.S.H.; Ashokkumar, V.; Cheng, C.K.; Park, Y.K.; Show, P.L. Microalgae and ammonia: A review on inter-relationship. *Fuel* **2021**, *303*, 121303. [[CrossRef](#)]
16. Kothari, R.; Ahmad, S.; Pathak, V.V.; Pandey, A.; Kumar, A.; Shankarayan, R.; Black, P.N.; Tyagi, V. Algal-based biofuel generation through flue gas and wastewater utilization: A sustainable prospective approach. *Biomass Convers. Biorefin.* **2021**, *11*, 1419–1442. [[CrossRef](#)]
17. Do, C.V.T.; Pham, M.H.T.; Pham, T.Y.T.; Dinh, C.T.; Bui, T.U.T.; Tran, T.D. Microalgae and bioremediation of domestic wastewater. *Curr. Opin. Green Sustain. Chem.* **2022**, *34*, 100595. [[CrossRef](#)]
18. Ahmed, S.F.; Mofijur, M.; Parisa, T.A.; Islam, N.; Kusumo, F.; Inayat, A.; Badruddin, I.A.; Khan, T.Y.; Ong, H.C. Progress and challenges of contaminate removal from wastewater using microalgae biomass. *Chemosphere* **2022**, *286*, 131656. [[CrossRef](#)]
19. Salbitani, G.; Carfagna, S. Ammonium utilization in microalgae: A sustainable method for wastewater treatment. *Sustainability* **2021**, *13*, 956. [[CrossRef](#)]
20. He, H.; Chen, Y.; Li, X.; Cheng, Y.; Yang, C.; Zeng, G. Influence of salinity on microorganisms in activated sludge processes: A review. *Int. Biodeterior. Biodegrad.* **2017**, *119*, 520–527. [[CrossRef](#)]
21. Latała, A.; Nędzi, M.; Stepnowski, P. Toxicity of imidazolium ionic liquids towards algae. Influence of salinity variations. *Green Chem.* **2009**, *12*, 60–64. [[CrossRef](#)]
22. von Alvensleben, N.; Magnusson, M.; Heimann, K. Salinity tolerance of four freshwater microalgal species and the effects of salinity and nutrient limitation on biochemical profiles. *J. Appl. Phycol.* **2016**, *28*, 861–876. [[CrossRef](#)]
23. Stoyneva, M.; Cocquyt, C.; Gärtner, G.; Vyverman, W. *Oocystis lacustris* CHOD. (Chlorophyta, Trebouxiophyceae) in Lake Tanganyika (Africa). *Linz. Biol. Beitr.* **2007**, *39*, 571–632.
24. Chuka-Ogwude, D.; Ogbonna, J.; Borowitzka, M.A.; Moheimani, N.R. Screening, acclimation and ammonia tolerance of microalgae grown in food waste digestate. *J. Appl. Phycol.* **2020**, *32*, 3775–3785. [[CrossRef](#)]
25. Oktem, Y.A.; Yuzer, B.; Aydin, M.I.; Okten, H.E.; Meric, S.; Selcuk, H. Chloride or sulfate? Consequences for ozonation of textile wastewater. *J. Environ. Manag.* **2019**, *247*, 749–755. [[CrossRef](#)]
26. Yaseen, D.; Scholz, M. Textile dye wastewater characteristics and constituents of synthetic effluents: A critical review. *Int. J. Environ. Sci. Technol.* **2019**, *16*, 1193–1226. [[CrossRef](#)]
27. OECD. Test No. 201: Freshwater alga and cyanobacteria, growth inhibition test. In *OECD Guidelines for the Testing of Chemicals, Section 2*; OECD Publishing: Paris, France, 2011.
28. Molins-Legua, C.; Meseguer-Lloret, S.; Moliner-Martinez, Y.; Campíns-Falcó, P. A guide for selecting the most appropriate method for ammonium determination in water analysis. *TrAC Trends Anal. Chem.* **2006**, *25*, 282–290. [[CrossRef](#)]
29. Holm-Hansen, O.; Riemann, B. Chlorophyll a determination: Improvements in methodology. *Oikos* **1978**, *30*, 438–447. [[CrossRef](#)]
30. Dai, R.; Li, Z.; Yan, F.; An, L.; Du, W.; Li, X. Evaluation of changes in *M. aeruginosa* growth and microcystin production under phosphorus starvation via transcriptomic surveys. *Sci. Total Environ.* **2023**, *893*, 164848. [[CrossRef](#)]
31. Stoyneva, M.P.; Ingolic, E.; Gärtner, G.; Vyverman, W. The pyrenoid ultrastructure in *Oocystis lacustris* CHODAT (Chlorophyta, Trebouxiophyceae). *Fottea* **2009**, *9*, 149–154. [[CrossRef](#)]
32. Mera, R.; Torres, E.; Abalde, J. Effects of sodium sulfate on the freshwater microalga *Chlamydomonas moewusii*: Implications for the optimization of algal culture media. *J. Phycol.* **2016**, *52*, 75–88. [[CrossRef](#)]
33. Lv, J.; Guo, J.; Feng, J.; Liu, Q.; Xie, S. Effect of sulfate ions on growth and pollutants removal of self-flocculating microalga *Chlorococcum* sp. GD in synthetic municipal wastewater. *Bioresour. Technol.* **2017**, *234*, 289–296. [[CrossRef](#)]
34. Bodnar, O.; Herts, A.; Herts, N.; Grubinko, V. The content of pigments and photosynthetic activity of *Chlorella vulgaris* Beij. (Chlorophyta) when exposed to sodium selenite, zinc sulphate, and chromium chloride. *Int. J. Algae* **2019**, *21*, 335–348. [[CrossRef](#)]
35. Shi, D.; Zhuang, K.; Chen, Y.; Xu, F.; Hu, Z.; Shen, Z. Effects of excess ammoniacal nitrogen (NH₄⁺-N) on pigments, photosynthetic rates, chloroplast ultrastructure, proteomics, formation of reactive oxygen species and enzymatic activity in submerged plant *Hydrilla verticillata* (L.f.) Royle. *Aquat. Toxicol.* **2020**, *226*, 105–160. [[CrossRef](#)] [[PubMed](#)]
36. Markou, G.; Depraetere, O.; Muylaert, K. Effect of ammonia on the photosynthetic activity of *Arthrospira* and *Chlorella*: A study on chlorophyll fluorescence and electron transport. *Algal Res.* **2016**, *16*, 449–457. [[CrossRef](#)]
37. Li, X.; Li, W.; Zhai, J.; Wei, H.; Wang, Q. Effect of ammonium nitrogen on microalgal growth, biochemical composition and photosynthetic performance in mixotrophic cultivation. *Bioresour. Technol.* **2019**, *273*, 368–376. [[CrossRef](#)]
38. Li, Y.; Chen, Y.-F.; Chen, P.; Min, M.; Zhou, W.; Martinez, B.; Zhu, J.; Ruan, R. Characterization of a microalga *Chlorella* sp. well adapted to highly concentrated municipal wastewater for nutrient removal and biodiesel production. *Bioresour. Technol.* **2011**, *102*, 5138–5144. [[CrossRef](#)]
39. Lv, J.; Wang, X.; Feng, J.; Liu, Q.; Nan, F.; Jiao, X.; Xie, S. Comparison of growth characteristics and nitrogen removal capacity of five species of green algae. *J. Appl. Phycol.* **2019**, *31*, 409–421. [[CrossRef](#)]
40. Tam, N.; Wong, Y. Effect of ammonia concentrations on growth of *Chlorella vulgaris* and nitrogen removal from media. *Bioresour. Technol.* **1996**, *57*, 45–50. [[CrossRef](#)]
41. Xin, L.; Hong-ying, H.; Ke, G.; Jia, Y. Growth and nutrient removal properties of a freshwater microalga *Scenedesmus* sp. LX1 under different kinds of nitrogen sources. *Ecol. Eng.* **2010**, *36*, 379–381. [[CrossRef](#)]

42. Han, L.; Pei, H.; Hu, W.; Han, F.; Song, M.; Zhang, S. Nutrient removal and lipid accumulation properties of newly isolated microalgal strains. *Bioresour. Technol.* **2014**, *165*, 38–41. [[CrossRef](#)]
43. Wang, M.; Kuo-Dahab, W.C.; Dolan, S.; Park, C. Kinetics of nutrient removal and expression of extracellular polymeric substances of the microalgae, *Chlorella* sp. and *Micractinium* sp., in wastewater treatment. *Bioresour. Technol.* **2014**, *154*, 131–137. [[CrossRef](#)]
44. Lachmann, S.C.; Mettler-Altmann, T.; Wacker, A.; Spijkerman, E. Nitrate or ammonium: Influences of nitrogen source on the physiology of a green alga. *Ecol. Evol.* **2019**, *9*, 1070–1082. [[CrossRef](#)]
45. Zhao, P.; Wang, Y.; Lin, Z.; Zhou, J.; Chai, H.; He, Q.; Li, Y.; Wang, J. The alleviative effect of exogenous phytohormones on the growth, physiology and gene expression of *Tetraselmis cordiformis* under high ammonia-nitrogen stress. *Bioresour. Technol.* **2019**, *282*, 339–347. [[CrossRef](#)]
46. Weber, S.; Grande, P.M.; Blank, L.M.; Klose, H. Insights into cell wall disintegration of *Chlorella vulgaris*. *PLoS ONE* **2022**, *17*, e0262500. [[CrossRef](#)]
47. Li, R.R.; Wang, B.L.; Nan, F.R.; Lv, J.P.; Liu, X.D.; Liu, Q.; Feng, J.; Xie, S.L. Effects of polystyrene nanoplastics on the physiological and biochemical characteristics of microalga *Scenedesmus quadricauda*. *Environ. Pollut.* **2023**, *319*, 120987. [[CrossRef](#)]
48. Ren, L.; Wang, M.R.; Wang, Q.C. ROS-induced oxidative stress in plant cryopreservation: Occurrence and alleviation. *Planta* **2021**, *254*, 124. [[CrossRef](#)]
49. Hnilickova, H.; Kraus, K.; Vachova, P.; Hnilicka, F. Salinity stress affects photosynthesis, malondialdehyde formation, and proline content in *Portulaca oleracea* L. *Plants* **2021**, *10*, 845. [[CrossRef](#)]
50. Zulfiqar, F.; Ashraf, M. Bioregulators: Unlocking their potential role in regulation of the plant oxidative defense system. *Plant Mol. Biol.* **2021**, *105*, 11–41. [[CrossRef](#)] [[PubMed](#)]
51. Han, Q.; Zheng, Y.; Qi, Q.; Peng, J.; Song, J.; Guo, J.; Guo, J. Involvement of oxidative stress in the sensitivity of two algal species exposed to roxithromycin. *Ecotoxicology* **2020**, *29*, 625–633. [[CrossRef](#)]
52. Baruah, P.; Chaurasia, N. Ecotoxicological effects of alpha-cypermethrin on freshwater alga *Chlorella* sp.: Growth inhibition and oxidative stress studies. *Environ. Toxicol. Pharmacol.* **2020**, *76*, 103347. [[CrossRef](#)] [[PubMed](#)]
53. Garcia-Caparros, P.; De Filippis, L.; Gul, A.; Hasanuzzaman, M.; Ozturk, M.; Altay, V.; Lao, M.T. Oxidative stress and antioxidant metabolism under adverse environmental conditions: A review. *Bot. Rev.* **2021**, *87*, 421–466. [[CrossRef](#)]
54. Zhang, S.; Bao, Q.; Huang, Y.; Han, N. Exogenous plant hormones alleviate As stress by regulating antioxidant defense system in *Oryza sativa* L. *Environ. Sci. Pollut. Res.* **2023**, *30*, 6454–6465. [[CrossRef](#)]
55. Hasanuzzaman, M.; Fujita, M. Plant oxidative stress: Biology, physiology and mitigation. *Plants* **2022**, *11*, 1185. [[CrossRef](#)] [[PubMed](#)]
56. Nam, S.H.; Il Kwak, J.; An, Y.J. Quantification of silver nanoparticle toxicity to algae in soil via photosynthetic and flow-cytometric analyses. *Sci. Rep.* **2018**, *8*, 292. [[CrossRef](#)] [[PubMed](#)]
57. Hindák, F.; Hindáková, A. Morphology and taxonomy of some rare chlorococcalean algae (Chlorophyta). *Biologia* **2008**, *63*, 781–790. [[CrossRef](#)]
58. Li, B.; Zhang, Y.; Xian, Y.; Luo, P.; Xiao, R.; Wu, J. Physiological response and tolerance of *Myriophyllum aquaticum* to a wide range of ammonium concentrations. *J. Environ. Manag.* **2022**, *317*, 115368. [[CrossRef](#)] [[PubMed](#)]
59. Tian, X.; Fang, Y.; Jin, Y.; Yi, Z.; Li, J.; Du, A.; He, K.; Huang, Y.; Zhao, H. Ammonium detoxification mechanism of ammonium-tolerant duckweed (*Landoltia punctata*) revealed by carbon and nitrogen metabolism under ammonium stress. *Environ. Pollut.* **2021**, *277*, 116834. [[CrossRef](#)] [[PubMed](#)]
60. Qiu, T.; Sun, Y.; Qu, T.; Xue, S.; Chen, J.; Zang, Y.; Liu, Q.; Tang, X. Study on gender differences between male and female *Sargassum thunbergii* based on metabolomic analysis and physiological functions. *Algal Res.* **2023**, *75*, 103267. [[CrossRef](#)]
61. Wang, J.; Chen, H.; Zhan, J.; Wang, Q. Ammonium nitrogen tolerant *Chlorella* strain screening and its damaging effects on photosynthesis. *Front. Microbiol.* **2019**, *9*, 429568. [[CrossRef](#)]
62. Heredia-Martínez, L.G.; Andrés-Garrido, A.; Martínez-Force, E.; Pérez-Pérez, M.E.; Crespo, J.L. Chloroplast damage induced by the inhibition of fatty acid synthesis triggers autophagy in *Chlamydomonas*. *Plant Physiol.* **2018**, *178*, 1112–1129. [[CrossRef](#)]
63. Yang, H.; Dong, B.; Wang, Y.; Qiao, Y.; Shi, C.; Jin, L.; Liu, M. Photosynthetic base of reduced grain yield by shading stress during the early reproductive stage of two wheat cultivars. *Sci. Rep.* **2020**, *10*, 14353. [[CrossRef](#)]

Disclaimer/Publisher’s Note: The statements, opinions and data contained in all publications are solely those of the individual author(s) and contributor(s) and not of MDPI and/or the editor(s). MDPI and/or the editor(s) disclaim responsibility for any injury to people or property resulting from any ideas, methods, instructions or products referred to in the content.